38. Hass R, C Kasper, S Bohm and R Jacobs. (2011). Different populations and sources of human mesenchymal stem cells (MSC): A comparison of adult and neonatal tissue-derived MSC. Cell Commun Signal 9:12.
39. Gustafsson MV, X Zheng, T Pereira, K Gradin, S Jin, J Lundkvist, JL Ruas, L Poellinger, U Lendahl and M Bondesson. (2005). Hypoxia requires notch signaling to maintain the undifferentiated cell state. Dev Cell 9:617-28.
40. Zheng X, S Linke, JM Dias, X Zheng, K Gradin, TP Wallis, BR Hamilton, M Gustafsson, JL Ruas, S Wilkins, RL Bilton, K Brismar, ML Whitelaw, T Pereira, JJ Gorman, J Ericson, DJ Peet, U Lendahl and L Poellinger. (2008). Interaction with factor inhibiting HIF-1 defines an additional mode of cross-coupling between the Notch and hypoxia signaling pathways. Proc Natl Acad Sci U S A 105:3368-73.
41. Pietras A, K von Stedingk, D Lindgren, S Pahlman and H Axelson. (2011). JAG2 induction in hypoxic tumor cells alters Notch signaling and enhances endothelial cell tube formation. Mol Cancer Res 9:626-36.
42. Bedogni B, JA Warneke, BJ Nickoloff, AJ Giaccia and MB Powell. (2008). Notch1 is an effector of Akt and hypoxia in melanoma development. J Clin Invest 118:3660-70.
43. Beitner-Johnson D, RT Rust, TC Hsieh and DE Millhorn. (2001). Hypoxia activates Akt and induces phosphorylation of GSK-3 in PC12 cells. Cell Signal 13:23-7.
44. Culver C, A Sundqvist, S Mudie, A Melvin, D Xirodimas and S Rocha. (2010). Mechanism of hypoxia-induced NF-kappaB. Mol Cell Biol 30:4901-21.
45. Rohwer N, C Dame, A Haugstetter, B Wiedenmann, K Detjen, CA Schmitt and T Cramer. (2010). Hypoxia-inducible factor 1alpha determines gastric cancer chemosensitivity via modulation of p53 and NF-kappaB. PLoS One 5:e12038.
46. Espinosa L, S Cathelin, T D'Altri, T Trimarchi, A Statnikov, J Guiu, V Rodilla, J Ingles-Esteve, J Nomdedeu, B Bellosillo, C Besses, O Abdel-Wahab, N Kucine, SC Sun, G Song, CC Mullighan, RL Levine, K Rajewsky, I Aifantis and A Bigas. (2010). The Notch/Hes1 pathway sustains NF-kappaB activation through CYLD repression in T cell leukemia. Cancer Cell 18:268-81.
47. Beverly LJ, DW Felsher and AJ Capobianco. (2005). Suppression of p53 by Notch in lymphomagenesis: implications for initiation and regression. Cancer Res 65:7159-68.
48. Kim SB, GW Chae, J Lee, J Park, H Tak, JH Chung, TG Park, JK Ahn and CO Joe. (2007). Activated Notch1 interacts with p53 to inhibit its phosphorylation and transactivation. Cell Death Differ 14:982-91.
49. Landor SK, AP Mutvei, V Mamaeva, S Jin, M Busk, R Borra, TJ Gronroos, P Kronqvist, U Lendahl and CM Sahlgren. (2011). Hypo- and hyperactivated Notch signaling induce a glycolytic switch through distinct mechanisms. Proc Natl Acad Sci U S A 108:18814-9.
50. Ciofani M and JC Zuniga-Pflucker. (2005). Notch promotes survival of pre-T cells at the beta-selection checkpoint by regulating cellular metabolism. Nat Immunol 6:881-8.
51. Welford SM, B Bedogni, K Gradin, L Poellinger, M Broome Powell and AJ Giaccia. (2006). HIF1alpha delays premature senescence through the activation of MIF. Genes Dev 20:3366-71.

52. Zhou D, J Xue, JC Lai, NJ Schork, KP White and GG Haddad. (2008). Mechanisms underlying hypoxia tolerance in Drosophila melanogaster: hairy as a metabolic switch. PLoS Genet 4:e1000221.
53. Funes JM, M Quintero, S Henderson, D Martinez, U Qureshi, C Westwood, MO Clements, D Bourboulia, RB Pedley, S Moncada and C Boshoff. (2007). Transformation of human mesenchymal stem cells increases their dependency on oxidative phosphorylation for energy production. Proc Natl Acad Sci U S A 104:6223-8.
54. Kawauchi K, K Araki, K Tobiume and N Tanaka. (2008). p53 regulates glucose metabolism through an IKK-NF-kappaB pathway and inhibits cell transformation. Nat Cell Biol 10:611-8.
55. Carter KL, E Cahir-McFarland and E Kieff. (2002). Epstein-barr virus-induced changes in B-lymphocyte gene expression. J Virol 76:10427-36.
56. Ak P and AJ Levine. (2010). p53 and NF-kappaB: different strategies for responding to stress lead to a functional antagonism. FASEB J 24:3643-52.
57. Prasad SM, M Czepiel, C Cetinkaya, K Smigielska, SC Weli, H Lysdahl, A Gabrielsen, K Petersen, N Ehlers, T Fink, SL Minger and V Zachar. (2009). Continuous hypoxic culturing maintains activation of Notch and allows long-term propagation of human embryonic stem cells without spontaneous differentiation. Cell Prolif 42:63-74.
58. Bash J, WX Zong, S Banga, A Rivera, DW Ballard, Y Ron and C Gelinas. (1999). Rel/NF-kappaB can trigger the Notch signaling pathway by inducing the expression of Jagged1, a ligand for Notch receptors. EMBO J 18:2803-11.

Figure legends

Figure 1. Hypoxia increases proliferation capacity and decreases senescence in hADMPCs. (A) Growth profiles of hADMPCs under normoxic (red square) and hypoxic (blue square) conditions. The population doubling level (PDL) was determined to be 0 when cells were isolated from human adipose tissue. Cells were maintained until they reached PDL13–15 (passage 3) and then split into four aliquots of equal cell densities. PDL was calculated based on the total cell number at each passage. **(B)** Detection of normoxic (Nx) and hypoxic (Hx) cells by flow cytometry following incorporation of EdU. **(C)** Percentages of apoptotic cells with sub-G1 DNA under Nx and Hx conditions. The results are presented as the mean of 3 independent experiments. **(D)** hADMPCs cultured under Nx and Hx conditions were harvested by trypsin-EDTA and then imaged using a phase-contrast microscope. Arrowheads indicate cells with a larger and more irregular shape. **(E)** Cells expanded under Nx and Hx conditions were stained with SA-β-gal. **(F)** Cellular ROS detection by the oxidative stress indicator CM-H2DCFDA in hADMPCs under Nx or Hx. Data are presented as the mean fluorescence intensity of 3 independent experiments. Error bars indicate SD. *$P < 0.05$ and **$P < 0.01$ indicate significant difference (independent *t*-test) between Nx and Hx. Scale bars; 100 μm.

Figure 2. Hypoxic culture maintains mesenchymal stem cell properties. hADMPCs cultured under normoxia (20% O_2) or hypoxia (5% O_2) were labeled with antibodies against the indicated antigens and analyzed by flow cytometry. Representative histograms are shown. The respective isotype control is shown as a gray line.

Figure 3. Hypoxic culture enhances stem cell properties. hADMPCs were expanded under normoxic and hypoxic conditions. **(A)** Normoxic (20% O_2) and hypoxic (5% O_2) cells at passage 8 were induced for 3 weeks to differentiate into osteoblasts and adipocytes and stained with alizarin red and Oil-red O, respectively. The stained dye was extracted and OD values were measured and plotted as the means of 3 independent experiments ± SD. *P < 0.05. Scale bars, 200 μm. **(B)** Normoxic (20% O_2) and hypoxic (5% O_2) cells at passage 8 were induced for 3 weeks to differentiate to chondrocytes, and immunofluorescent analysis of collagen II (red) and Alucian blue staining were performed. The blue signals indicate nuclear staining. Scale bars, 100 μm. Non-induced control cultures in growth medium without adipogenic, osteogenic or chondrogenic differentiation stimuli are shown (Undifferentiated).

Figure 4. Hypoxic culture condition activates Notch signaling but not HIF proteins. hADMPCs were expanded under normoxic (20% O_2) and hypoxic (5% O_2) conditions. DAPT (1 μM) was added to inhibit Notch signaling. **(A)** Western blot analysis of intracellular domain of Notch1 (Notch1 ICD) expression. Actin served as the loading control. Numbers below blots indicate relative band intensities as determined by ImageJ software. (**B**) Q-PCR analysis of *HES1*. Each expression value was calculated with the ΔΔCt method using *UBE2D2* as an internal control. (**C**) Western blot analysis of HES1 in nuclear fractions of hADMPCs. Lamin A/C served as the loading control. **(D, E)** Western blot analysis of HIF-1α (**D**) and HIF-2α (**E**). Cobalt chloride ($CoCl_2$) was added at a concentration of 100 μM to stabilize HIF proteins (positive control). (**F**) Western blot analysis of phosphorylated

Akt (p-Akt) and Akt. Actin served as the loading control. Numbers below blots indicate relative band intensities as determined by ImageJ software. (**G**) Western blot analysis of nuclear localization of p65. Lamin A/C served as the loading control. Numbers below blots indicate relative band intensities as determined by ImageJ software. (**H**) Western blot analysis of phosphorylated p53 (p-p53) and p53. Actin served as the loading control. (**I**) Activity of p53 was measured by the p53-luciferase reporter assay. Relative luciferase activity was determined from 3 independent experiments and normalized to pGL4.74 activity.

Figure 5. Notch signaling is indispensable for acquisition of the advantageous properties of hADMPCs. hADMPCs were expanded under normoxic (20% O_2; Nx) and hypoxic (5% O_2; Hx) conditions. DAPT (1 μM) was added to inhibit Notch signaling. **(A)** Growth profiles of hADMPCs under Nx (red) and Hx (blue) conditions. Solid lines represent control cells and dotted lines represent DAPT-treated cells. The number of population doublings was calculated based on the total cell number at each passage. **(B)** Percentages of apoptotic cells with sub-G1 DNA. Results are presented as the mean of 3 independent experiments ± SD. **(C-D)** hADMPCs at passage 8 were induced for 3 weeks to differentiate into adipocytes **(C)** and osteoblasts **(D)** and stained with Oil Red O and Alizarin Red, respectively. The stained dye was extracted, and OD values were measured and plotted as the means of 3 independent experiments ± SD. **(E)** hADMPCs at passage 8 were induced for 3 weeks to differentiate into chondrocytes, and an immunofluorescent analysis of collagen II (red) was performed. The blue signals indicate nuclear staining. **(F)** hADMPCs were stained with SA-β-gal. *$P < 0.05$ and **$P < 0.01$ indicate significant difference (independent *t*-test) between Nx and Hx. Scale bars; 100 μm.

Figure 6. Glycolysis is enhanced under 5% oxygen through Notch signaling. (A-D) hADMPCs were expanded under normoxic (20% O_2) and hypoxic (5% O_2) conditions. DAPT (1 μM) was added in to inhibit Notch signaling. **(A)** Glucose consumption and lactate production of hADMPCs were measured and plotted as the means of 3 independent experiments ± SD. **(B)** Relative mRNA expression of *SLC2A3*, *TPI, PGK1, TIGAR*, and *SCO2* in hADMPCs. Each expression value was calculated with the ΔΔCt method using *UBE2D2* as an internal control. **(C, D)** Hexokinase (HK), phosphofructokinase (PFK), lactate dehydrogenase (LDH) (**C**), pyruvate dehydrogenase (PDH), and Complex IV (Cox IV) (**D**) activities were measured and the value of relative activity was plotted as the means of 3 independent experiments ± SD. **(E, F)** hADMPCs were transduced with either mock (Cont) or HES1 and then cultured for 3 days. **(E)** Relative mRNA expression of *SLC2A3*, *TPI, PGK1, TIGAR*, and *SCO2* in hADMPCs. Each expression value was calculated with the ΔΔCt method using *UBE2D2* as an internal control. **(F)** Glucose consumption and lactate production of hADMPCs were measured and plotted as the means of 3 independent experiments ± SD. **(G)** hADMPCs were transduced with either scrambled control RNAi (Cont) or RNAi against HES1 (HES1-KD), and then cultured for 3 days. Glucose consumption and lactate production of hADMPCs were measured and plotted as the means of 3 independent experiments ± SD. **P < 0.01. * 0.01 < P < 0.05.

Figure 7. Glycolysis supports proliferation of hADMPCs. hADMPCs were treated with 0, 0.2, 0.4 and 1 mM 2-deoxy-D-glucose (2-DG) **(A)** or 0, 1 and 5 mM sodium azide (NaN_3) **(B)** for 24 h. Cells were then allowed to

incorporate EdU for 2 h, and the EdU-positive cells were analyzed by flow cytometry. The percentages for the 0 mM control were plotted as the means of 3 independent experiments ± SD. ** $P < 0.01$. * $0.01 < P < 0.05$.

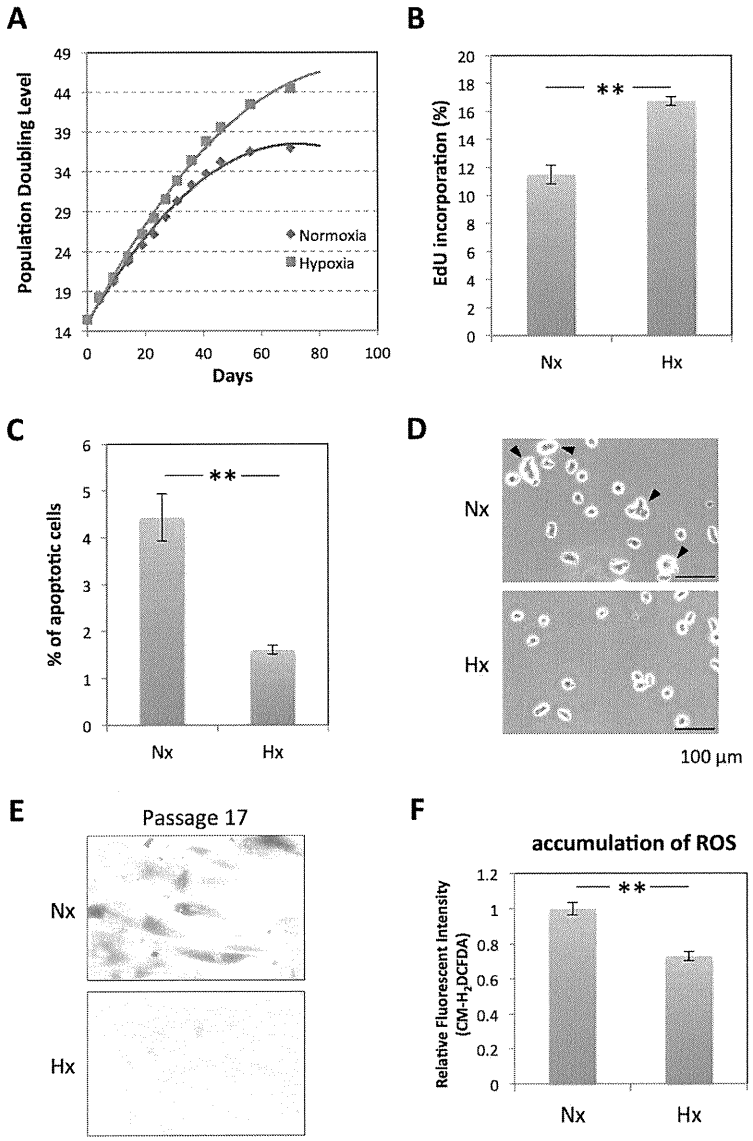

MoriyamaFig1
170x237mm (300 x 300 DPI)

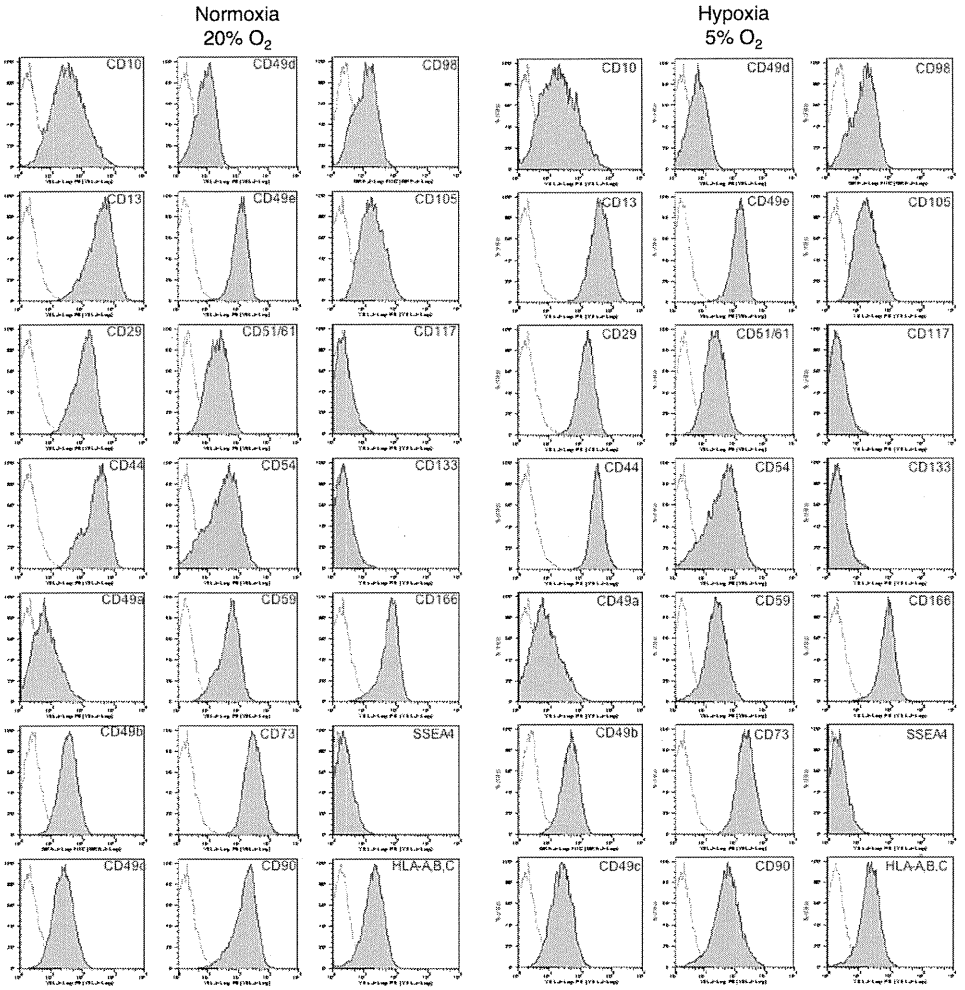

MoriyamaFig2
169x174mm (300 x 300 DPI)

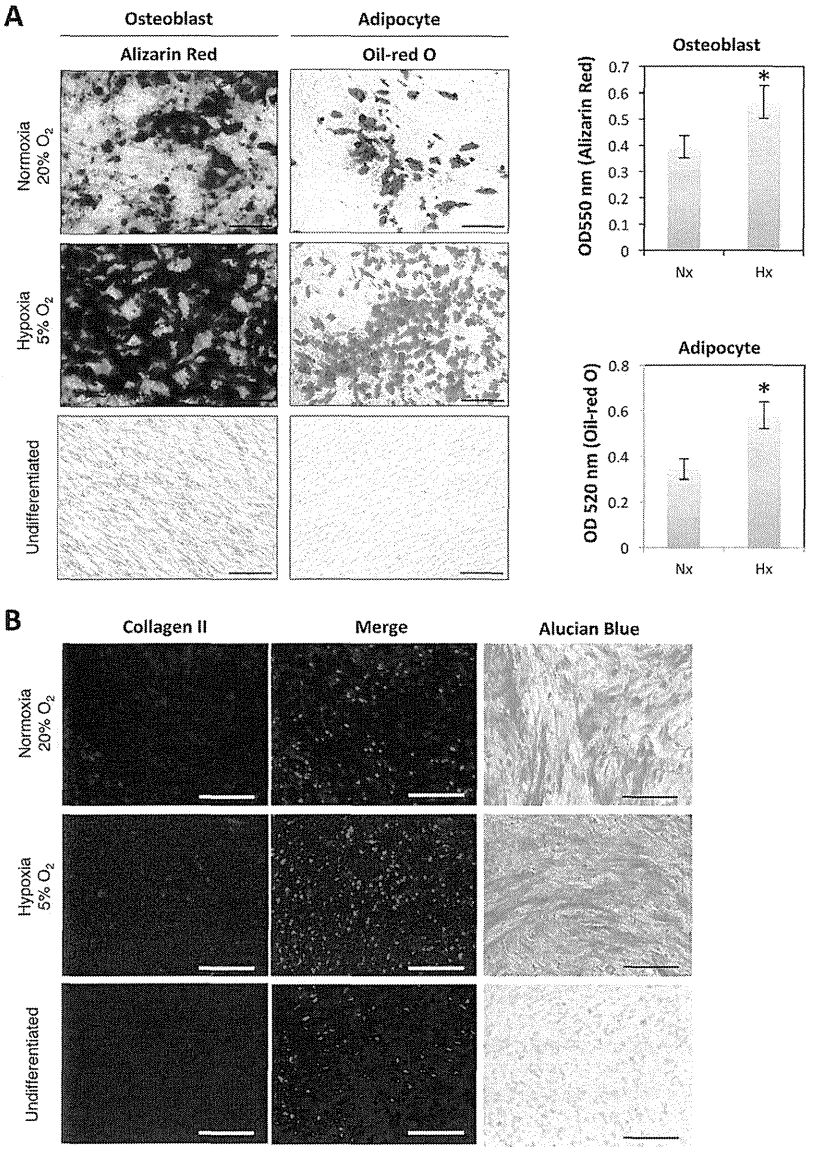

Figure 3
101x144mm (300 x 300 DPI)

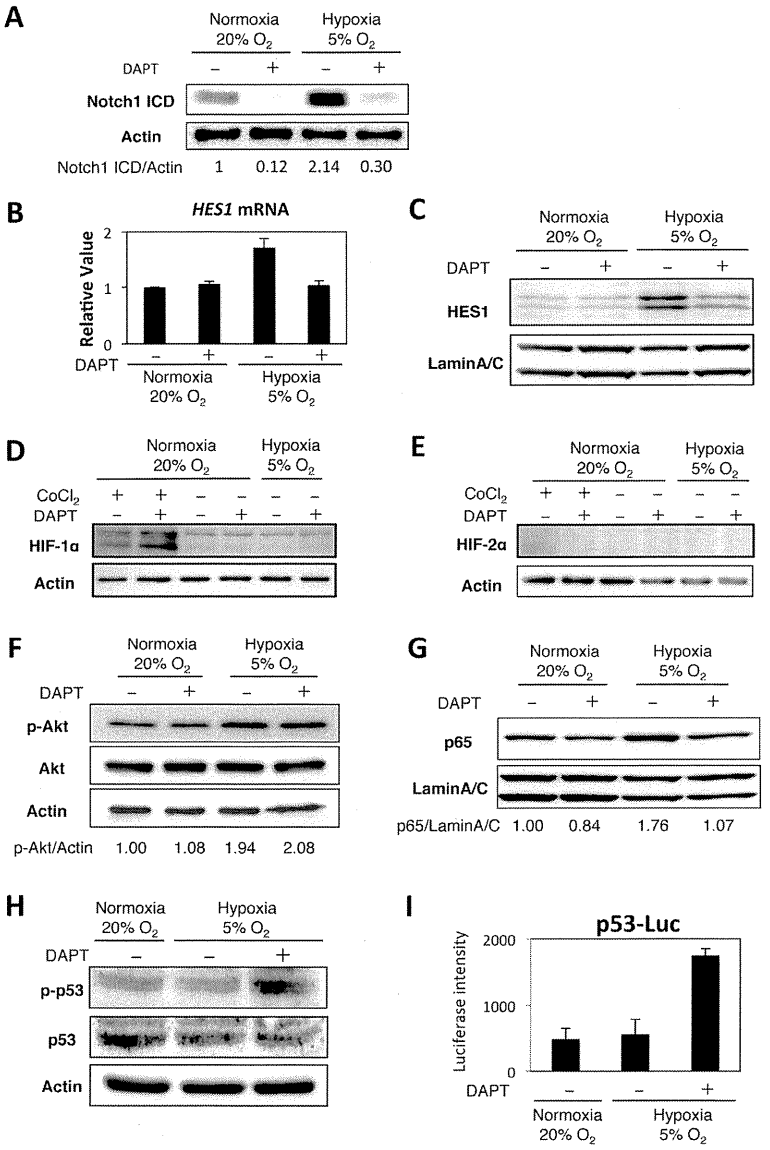

MoriyamaFig4
163x246mm (300 x 300 DPI)

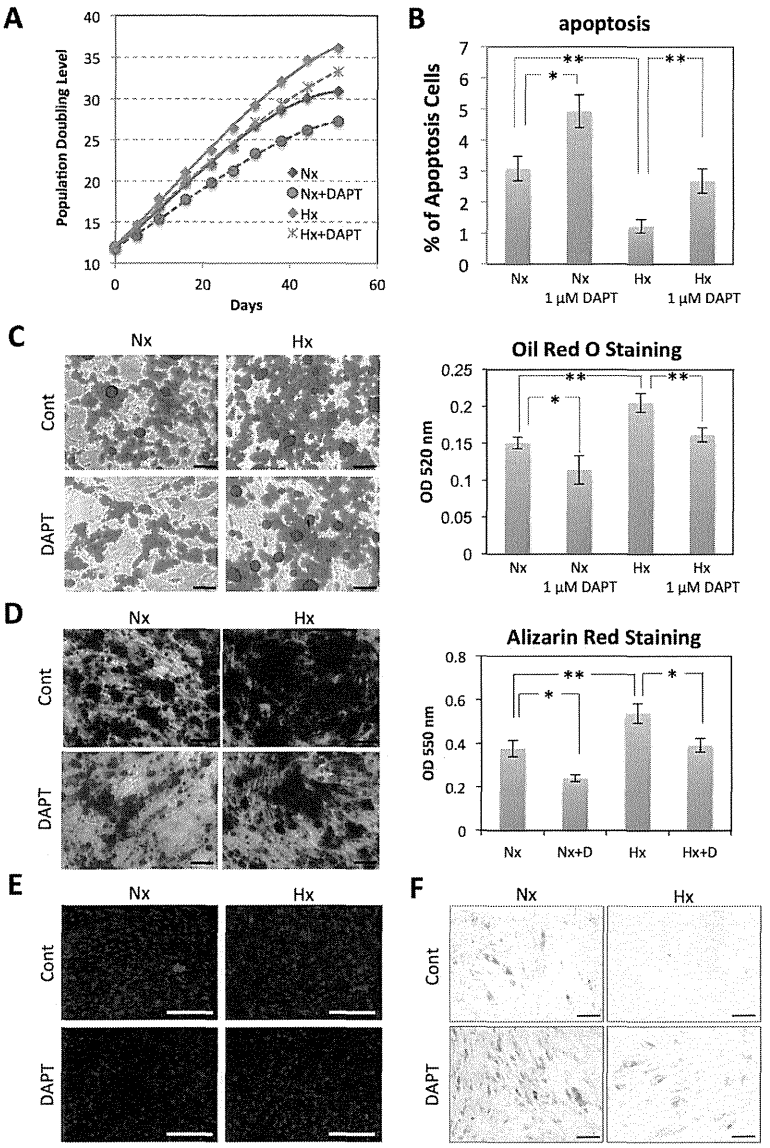

MoriyamaFig5
171x247mm (300 x 300 DPI)

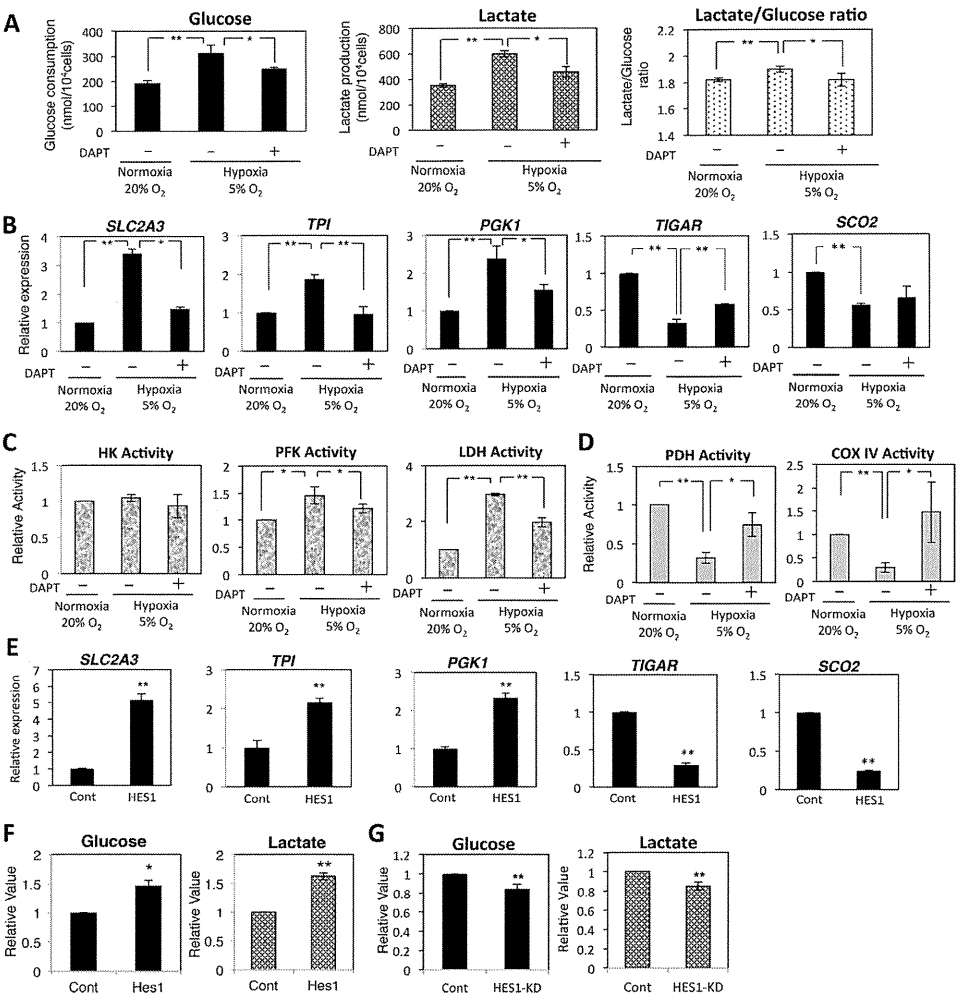

MoriyamaFig6
169x176mm (300 x 300 DPI)

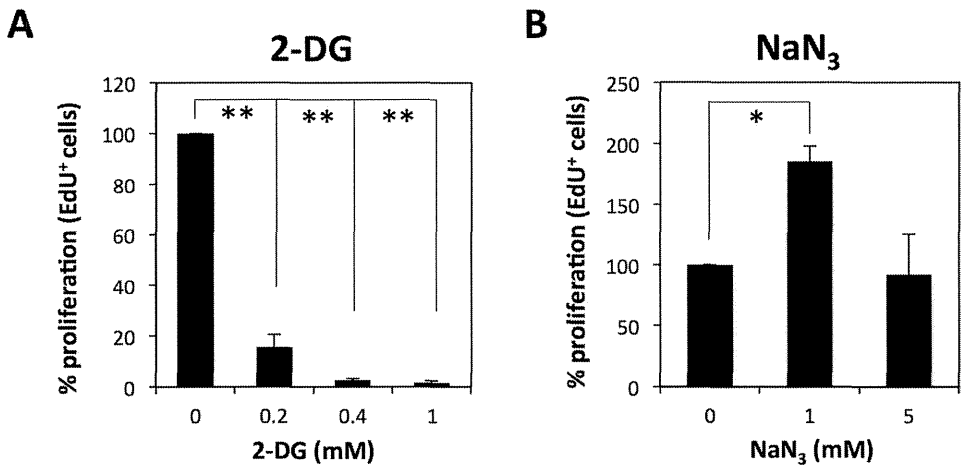

MoriyamaFig7
151x72mm (300 x 300 DPI)

OPEN ACCESS Freely available online

PLOS ONE

Tightly Regulated and Homogeneous Transgene Expression in Human Adipose-Derived Mesenchymal Stem Cells by Lentivirus with Tet-Off System

Hiroyuki Moriyama[1*ϑ], Mariko Moriyama[1,2ϑ], Kei Sawaragi[1], Hanayuki Okura[2], Akihiro Ichinose[3], Akifumi Matsuyama[2], Takao Hayakawa[1]

1 Pharmaceutical Research and Technology Institute, Kinki University, Higashi-Osaka, Osaka, Japan, **2** Platform for Realization of Regenerative Medicine, Foundation for Biomedical Research and Innovation, Chuo-ku, Kobe, Hyogo, Japan, **3** Department of Plastic Surgery, Kobe University Hospital, Chuo-ku, Kobe, Hyogo, Japan

Abstract

Genetic modification of human adipose tissue–derived multilineage progenitor cells (hADMPCs) is highly valuable for their exploitation in therapeutic applications. Here, we have developed a novel single tet-off lentiviral vector platform. This vector combines (1) a modified tetracycline (tet)-response element composite promoter, (2) a multi-cistronic strategy to express an improved version of the tet-controlled transactivator and the blasticidin resistance gene under the control of a ubiquitous promoter, and (3) acceptor sites for easy recombination cloning of the gene of interest. In the present study, we used the cytomegalovirus (CMV) or the elongation factor 1 α (EF-1α) promoter as the ubiquitous promoter, and EGFP was introduced as the gene of interest. hADMPCs transduced with a lentiviral vector carrying either the CMV promoter or the EF-1α promoter were effectively selected by blasticidin without affecting their stem cell properties, and EGFP expression was strictly regulated by doxycycline (Dox) treatment in these cells. However, the single tet-off lentiviral vector carrying the EF-1α promoter provided more homogenous expression of EGFP in hADMPCs. Intriguingly, differentiated cells from these Dox-responsive cell lines constitutively expressed EGFP only in the absence of Dox. This single tet-off lentiviral vector thus provides an important tool for applied research on hADMPCs.

Citation: Moriyama H, Moriyama M, Sawaragi K, Okura H, Ichinose A, et al. (2013) Tightly Regulated and Homogeneous Transgene Expression in Human Adipose-Derived Mesenchymal Stem Cells by Lentivirus with Tet-Off System. PLoS ONE 8(6): e66274. doi:10.1371/journal.pone.0066274

Editor: Niels Olsen Saraiva Câmara, Universidade de Sao Paulo, Brazil

Received December 20, 2012; **Accepted** May 2, 2013; **Published** June 12, 2013

Funding: This work was supported in part by MEXT KAKENHI Grant Number 23791304 to M.M. and 24791927 to H.M. This work was also supported in part by grants from the Ministry of Health, Labor, and Welfare of Japan and a grant from the Program for Promotion of Fundamental Studies in Health Sciences of the National Institute of Biomedical Innovation (NIBIO). The funders had no role in study design, data collection and analysis, decision to publish, or preparation of the manuscript.

Competing Interests: The authors have declared that no competing interests exist.

* E-mail: moriyama@phar.kindai.ac.jp

ϑ These authors contributed equally to this work.

Introduction

Human adipose tissue–derived mesenchymal stem cells (MSCs), also referred to as human adipose tissue–derived multilineage progenitor cells (hADMPCs), are multipotent stem cells that can differentiate into various types of cells, including hepatocytes [1], cardiomyoblasts [2], pancreatic cells [3], and neuronal cells [4–6]. They can be easily and safely obtained from lipoaspirates without posing serious ethical issues and can also be expanded ex vivo under appropriate culture conditions. Moreover, MSCs, including hADMPCs, have the ability to migrate to injured areas and secrete a wide variety of cytokines and growth factors necessary for tissue regeneration [7–11]. Because of their hypoimmunogenicity and immune modulatory effects, hADMPCs are good candidates for gene delivery vehicles for therapeutic purposes [12]. Thus, hADMPCs are an attractive material for cell therapy and tissue engineering, making the development of technologies for permanent and highly controlled genetic modification of hADMPCs quite valuable.

Lentiviral vectors are powerful tools for gene transfer in primary human cells, as they integrate into the host cell genome, resulting in stable long-term transgene expression. Lentiviral vectors are less prone to transcriptional silencing than oncoretroviral vectors [13,14]; however, researchers have reported that transgene silencing occurs when a strong promoter, such as the cytomegalovirus (CMV) promoter, is used in certain cell types, especially embryonic stem cells [15–17]. Recently, it has been reported that the CMV promoter is also silenced in rat bone marrow–derived MSCs [18,19], suggesting that consideration of promoter used in the lentiviral vector is one of the most critical issues.

In addition to the choice of promoters, the specific gene expression system can have a great impact on the properties and functions of the infected hADMPCs. In order to express therapeutic genes, master regulatory genes, or microRNAs, the development of a tightly regulated, inducible gene expression system is required. The tetracycline (tet)-regulated transgene expression (tet-off) system is the most advanced system being used in gene therapy trials [20]. Two expression cassettes need to be delivered for use of the tet-off system: the regulatory unit for the constitutive expression of the transactivator (tTA), and the tet-controlled responsive unit for the expression of the gene of interest. Traditionally, these 2 cassettes should be transduced separately to establish tet-inducible cell lines. This time-consuming process

significantly limits the number of cell lines that can be generated for target gene expression. Recently, several researchers attempted to develop single-vector–based tet-inducible lentiviral systems [21–24]. However, the large plasmid size and lack of antibiotic selectable markers in these systems made the generation of plasmid constructs, high titer lentiviral particles, and stably expressing transgenic cell lines difficult.

To overcome the limitations of the current single vector-based tet-inducible lentiviral systems, we generated a robust system that incorporates all the necessary components for tet-off gene expression, restriction enzyme treatment/ligation independent cloning system, and antibiotic selectable markers in a single lentiviral vector. This vector consists of a modified tet-response element composite promoter (TRE-Tight) followed by a Gateway cassette containing *att*R recombination sites flanking a *ccd*B gene and a chloramphenicol resistant gene, which allows for easy and rapid shuttling of the gene of interest into the vector. This vector also carries an improved version of the tet-controlled transactivator (tTA-advanced) and the blasticidin resistance gene, linked by the self-cleaving viral T2A peptide, under a ubiquitous promoter. In the present study, we examined 2 ubiquitous promoters commonly used in mammalian systems: the CMV promoter and the human polypeptide chain elongation factor 1 α (EF-1α) promoter, to determine which promoter is more efficient in hADMPCs. In addition, we also confirmed whether genetically modified hADMPCs maintained their stem cell properties following transduction with this single tet-off lentiviral vector. We examined the expression pattern of cell surface markers, as well as the cells' differentiation potential into adipocytes, chondrocytes, osteocytes, and neuronal cells. Our data demonstrated that hADMPCs transduced with our all-in-one lentiviral vector were effectively selected by blasticidin without affecting their stem cell properties, and transgene expression was strictly regulated by doxycycline (Dox) not only in undifferentiated cells but also in differentiated cells. A single tet-off lentiviral vector system thus provides a powerful tool for applied research on hADMPCs.

Materials and Methods

Adipose Tissue Samples

Subcutaneous adipose tissue samples (10–50 g each) were resected during plastic surgery in 5 women (age, 20–60 years) as excess discards. The study protocol was approved by the Review Board for Human Research of Kobe University Graduate School of Medicine, Foundation for Biomedical Research and Innovation, and Kinki University Pharmaceutical Research and Technology Institute (reference number: 10-005). Each subject provided signed informed consent.

Cell Culture

hADMPCs were isolated as previously reported [1,11,25,26] and maintained in a medium containing 60% DMEM-low glucose, 40% MCDB-201 medium (Sigma Aldrich, St. Louis, MO, USA), 1× insulin-transferrin-selenium (Life technologies, Carlsbad, CA, USA), 1 nM dexamethasone (Sigma Aldrich, St. Louis, MO, USA), 100 mM ascorbic acid 2-phosphate (Wako, Osaka, Japan), 10 ng/mL epidermal growth factor (PeproTech, Rocky Hill, NJ, USA), and 5% fetal bovine serum. The cells were plated to a density of 5×10^3 cells/cm^2 on fibronectin-coated dishes, and the medium was replaced every 2 days.

Plasmid Construction and Lentivirus Production

EGFP was cloned into a pENTR11 vector (Invitrogen) to create an entry vector, pENTR11-EGFP. To generate pTRE-RfA, the tet-responsive element (TRE) of the pTRE-Tight vector (Clontech, Mountain Veiw, CA, USA) and the Reading frame A (RfA), a Gateway cassette containing *att*R recombination sites flanking a *ccd*B gene and a chloramphenicol-resistance gene (Invitrogen) were introduced into *Xba*I-*Xho*I sites of pSico (Addgene plasmid 11578). An improved version of the tet-controlled transactivator (tTA-advanced: pTet-off-advanced Clontech) was linked to the blasticidin resistance (Bsd) gene by the viral T2A peptide to generate tTA-2A-Bsd. Briefly, 2A-Bsd was amplified by PCR using the following primers:

2A-Bsd F: GGGGGATCCGGCGAGGGCAGAGGAAGTCTTCTAACATGCGGTGACGTGGAGGAAAATCCCGGGCCCATGAAGACCTTCAACATCTCTCAG, Bsd R: GCGAGATCTTTAGTTCCTGGTGTACTTG. The resultant product was confirmed by sequencing and ligation with the SmaI site of tTA. EF promoter/CMV promoter and tTA-2A-Bsd was introduced into pTRE-RfA to produce pTRE-RfA-EF-tTA-2A-Bsd or pTRE-RfA-CMV-tTA-2A-Bsd. The entry vector pENTR11-EGFP and pTRE-RfA-EF-tTA-2A-Bsd, pTRE-RfA-CMV-tTA-2A-Bsd, CSII-EF-RfA, or CSII-CMV-RfA (kindly provided by Dr. Miyoshi, RIKEN BioResource Center, Tsukuba, Japan) were incubated with LR clonase II enzyme mix (Invitrogen) to generate pTRE-EGFP-EF-tTA-2A-Bsd, pTRE-EGFP-CMV-tTA-2A-Bsd, CSII-EF-EGFP or CSII-CMV-EGFP. The resultant plasmid was mixed with packaging plasmids (pCAG-HIVg/p and pCMV-VSVG-RSV-Rev, kindly provided by Dr. Miyoshi) and transfected into 293T cells. The supernatant medium, which contained lentiviral vectors, was collected 2 days after transduction and concentrated by centrifugation (6000× *g*, 15 h, 4°C). Viral titers (transduction unit: TU) were determined by serial dilution on 293T cells and the percentage of EGFP positive cells was measured by Guava easyCyte 8HT flow cytometer (Merck-Millipore, Billerica, MA, USA).

Plasmid Propagation in *E. coli*

DH5α (F-, Φ80dlacZΔM15, Δ(lacZYA-argF)U169, deoR, recA1, endA1, hsdR17(rK-, mK+), phoA, supE44, λ-, thi-1, gyrA96, relA1) were used for general purpose. To propagate plasmids containing the ccdB gene, One Shot® ccdB Survival™ 2 T1 Phage-Resistant (T1R) chemically competent *E. coli* (Invitrogen) were used.

Western Blot Analysis

Cells were washed with ice-cold phosphate-buffered saline and lysed with M-PER Mammalian Protein Extraction Reagent (Thermo Scientific Pierce, Rockford, IL, USA). Equal amounts of proteins were separated by sodium dodecyl sulfate polyacrylamide gel electrophoresis, transferred to polyvinylidene fluoride membranes (Immobilon-P; Merck-Millipore), and probed with antibody against TetR (from Clontech). Horseradish peroxidase (HRP)-conjugated anti-mouse secondary antibody (Cell Signaling Technology, Danvers, MA, USA) was used as a probe, and immunoreactive bands were visualized with the Immobilon Western Chemiluminescent HRP substrate (Millipore). The band intensity was measured using ImageJ software.

Flow Cytometry Analysis

hADMPCs were seeded at a density of 2×10^4 cells per well in 12-well culture plates and were transduced with CSII-EF-EGFP or CSII-CMV-EGFP at a multiplicity of infection (m.o.i.) of 25, 50,

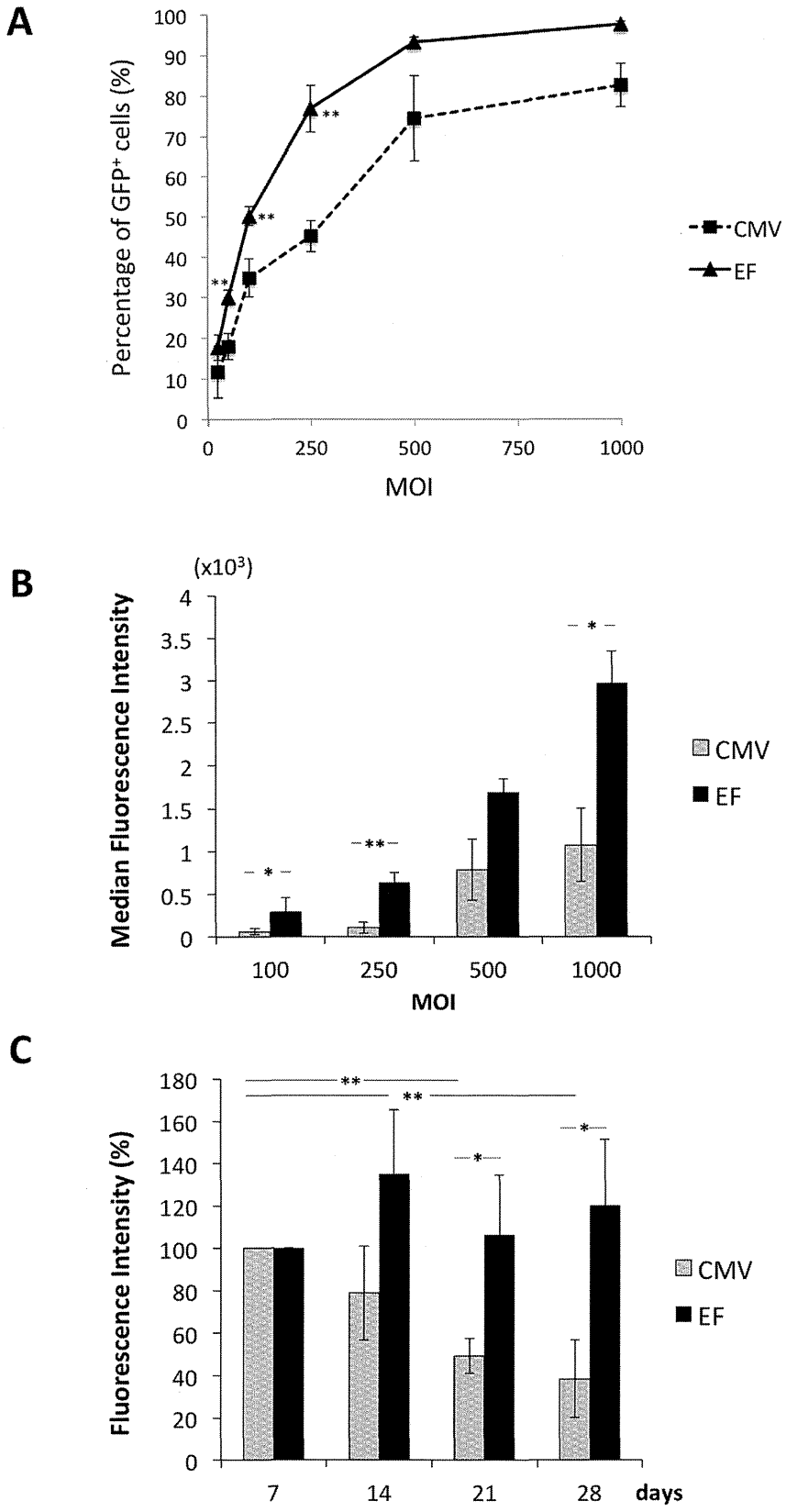

Figure 1. The efficiency of CMV or EF-1α promoter in hADMPCs. Lentiviral vectors encoding EGFP under the control of CMV or EF-1α promoter were transduced with hADMPCs at m.o.i. of 25, 50, 100, 250, 500, and 1000, and the cells were analyzed by flow cytometry. (A) The percentage of EGFP-positive hADMPCs transduced with CSII-CMV-EGFP (CMV) or CSII-EF-EGFP (EF). (B) (C) The median fluorescence intensities of the

EGFP-expressing populations. (B) hADMPCs transduced with CSII-CMV-EGFP or CSII-EF-EGFP at m.o.i. of 100, 250, 500, and 1000 were analyzed. (C) hADMPCs transduced with CSII-CMV-EGFP or CSII-EF-EGFP at m.o.i. of 1000 were analyzed over a 28 day period. Error bars represent the standard error of 3 independent analyses. **, $P<0.01$; *, $P<0.05$ (Student's t test).
doi:10.1371/journal.pone.0066274.g001

100, 250, 500, and 1000. Four days later, the cells were analyzed with a Guava easyCyte 8HT flow cytometer (Merck-Millipore) using an argon laser at 488 nm. Dead cells were excluded with the LIVE/DEAD fixable far red dead cell stain kit (Invitrogen). For analysis of hADMPCs transduced with pTRE-EGFP-EF-tTA-2A-Bsd or pTRE-EGFP-CMV-tTA-2A-Bsd, hADMPCs were transduced with the lentiviral vector at a m.o.i. of 250 and were cultured with or without 1 μg/mL Dox. Four days later, a part of the cells were analyzed with a Guava easyCyte 8HT flow cytometer. The rest of the cells were cultured with 4 μg/mL blasticidin and 1 μg/mL Dox for 3 weeks. Then, the cells were seeded in 6-well plates and cultured with or without Dox for 4 days. The cells were harvested and re-suspended in staining buffer (PBS containing 1% BSA, 2 mM EDTA, and 0.01% sodium azide) at a density of 1×10^6 cells/mL and incubated with phycoerythrin (PE)-conjugated antibody against CD13, CD29, CD34, CD44, CD73, CD90, CD105, or CD166 for 20 min. Non-specific staining was assessed using relevant isotype controls. 525/30 nm and 583/26 nm band pass filters were used for the detection of EGFP and PE, respectively. Dead cells were excluded with the LIVE/DEAD fixable far red dead cell stain kit (Invitrogen). FlowJo software (TreeStar Inc., Ashland, OR, USA) was used for quantitation analysis. The threshold for gating was determined as the fluorescence value above which less than 1% of the control cells were considered as positive events.

Fluorescence Microscopy

Phase contrast and fluorescence images were obtained using Fluorescence Microscope (BZ-9000; Keyence, Osaka, Japan) using BZ Analyzer Software (Keyence).

Adipogenic, Osteogenic, Chondrogenic, and Neurogenic Differentiation Procedures

For adipogenic differentiation, cells were cultured in differentiation medium (Zen-Bio, Durham, NC, USA). After 3 days, half of the medium was changed to adipocyte medium (Zen-Bio), and this was repeated every 3 days. Three weeks after differentiation, characterization of adipocytes was confirmed by microscopic observation of intracellular lipid droplets by oil red O staining. Osteogenic differentiation was induced by culturing the cells in DMEM containing 10 nM dexamethasone, 50 mg/dL ascorbic acid 2-phosphate, 10 mM β-glycerophosphate (Sigma), and 10% FBS. Differentiation was examined by alizarin red staining. For chondrogenic differentiation, 2×10^5 hADMPCs were centrifuged at $400\times g$ for 10 min. The resulting pellets were cultured in chondrogenic medium (α-MEM supplemented with 10 ng/mL transforming growth factor-β, 10 nM dexamethasone, 100 mM ascorbate, and 1× insulin–transferrin–selenium solution) for 14 days, as described previously [27]. The pellets were fixed with 4% paraformaldehyde in PBS, embedded in OCT, frozen, and sectioned at 8 μm. The sections were incubated with PBSMT (PBS containing 0.1% Triton X-100, 2% skim milk) for 1 h at room temperature, and then incubated with mouse monoclonal antibody against type II collagen (Abcam, Cambridge, MA, USA) and rabbit polyclonal antibody against GFP (Invitrogen) for 1 h. After washing with PBS, cells were incubated with Alexa 546 conjugated anti-mouse IgG and Alexa 488 conjugated anti-rabbit IgG for chondrocytes (Invitrogen) or Alexa 546 conjugated anti-rabbit IgG and Alexa 488 conjugated anti-rat IgG (Invitrogen) for neuronal cells. The cells were counterstained with 4′-6-diamidino-2-phenylindole (DAPI) (Invitrogen) to identify cellular nuclei. For neurogenic differentiation, cells were cultured in Hyclone AdvanceSTEM neural differentiation medium (Thermo Scientific, South Logan, UT, USA) for 2 days. Differentiation was examined by immunofluorescent staining against β3-tubulin. Cells were fixed with 4% paraformaldehyde in PBS for 10 min at 4°C and then washed 3 times in PBS. Blocking was performed with PBSMT for 1 h at room temperature. The differentiated cells were incubated with rabbit monoclonal antibody against β3-tubulin (Cell Signaling Technologies, Danvers, MA, USA) and rat monoclonal antibody against GFP (Nacalai, Kyoto, Japan). After washing with PBS, cells were incubated with Alexa 546 conjugated anti-rabbit IgG and Alexa 488 conjugated anti-rat IgG (Invitrogen). The cells were counterstained with 4′-6-diamidino-2-phenylindole (DAPI) (Invitrogen) to identify cellular nuclei.

Results

The Efficiency of the EF-1α Promoter was Higher than that of the CMV Promoter in hADMPCs

To determine the efficiency of the EF-1α promoter and the CMV promoter, hADMPCs were transduced with CSII-EF-EGFP or CSII-CMV-EGFP at a m.o.i. of 25, 50, 100, 250, 500, and 1000 and analyzed by flow cytometry. As shown in Figure 1A, percentage of GFP-positive cells increased in a dose-dependent manner. Intriguingly, transduction efficiency of CSII-EF-EGFP was significantly higher than that of CSII-CMV-EGFP in hADMPCs (Figure 1A). Moreover, a higher induction level of GFP was observed under the EF-1α promoter than under the CMV promoter, based on the median fluorescent intensity (Figure 1B). Furthermore, GFP fluorescent intensities driven from the CMV promoter were significantly decreased (from 100% on day 7 to 49.3% on day 21 and 38.4% on day 28; Figure 1C), indicating that promoter silencing occurred as previously reported [19]. In contrast, hADMPCs transduced with CSII-EF-EGFP sustained GFP expression levels with no significant reduction throughout the 28-day experimental period (Figure 1C).

Construction and Characterization of Dual-promoter Lentiviral Vectors in hADMPCs

Next, we constructed dual-promoter lentiviral vectors, which contain TRE-Tight followed by an improved version of tet-controlled transactivator (tTA advanced) induced under the CMV or EF-1α promoter (Figure 2A). In this "single tet-off lentiviral vector platform", the regulator and response elements are combined in a single lentiviral genome, along with a Gateway cassette containing *att*R recombination sites flanking a *ccd*B gene and a chloramphenicol-resistance gene, which allows an easy and rapid shuttling of the gene of interest into the vectors using the Gateway LR recombination reaction (Figure 2A). Using this system, we constructed pTRE-EGFP-CMV-tTA-2A-Bsd or pTRE-EGFP-EF-tTA-2A-Bsd (Figure 2B). Both the CMV and the EF-1α promoters drive the mRNA expression of tTA advanced linked to the Bsd gene by the Thosea asigna virus 2A (T2A) peptide sequence. This single transcript is then translated and cleaved into 2 proteins; tTA advanced carrying 2A tag at the

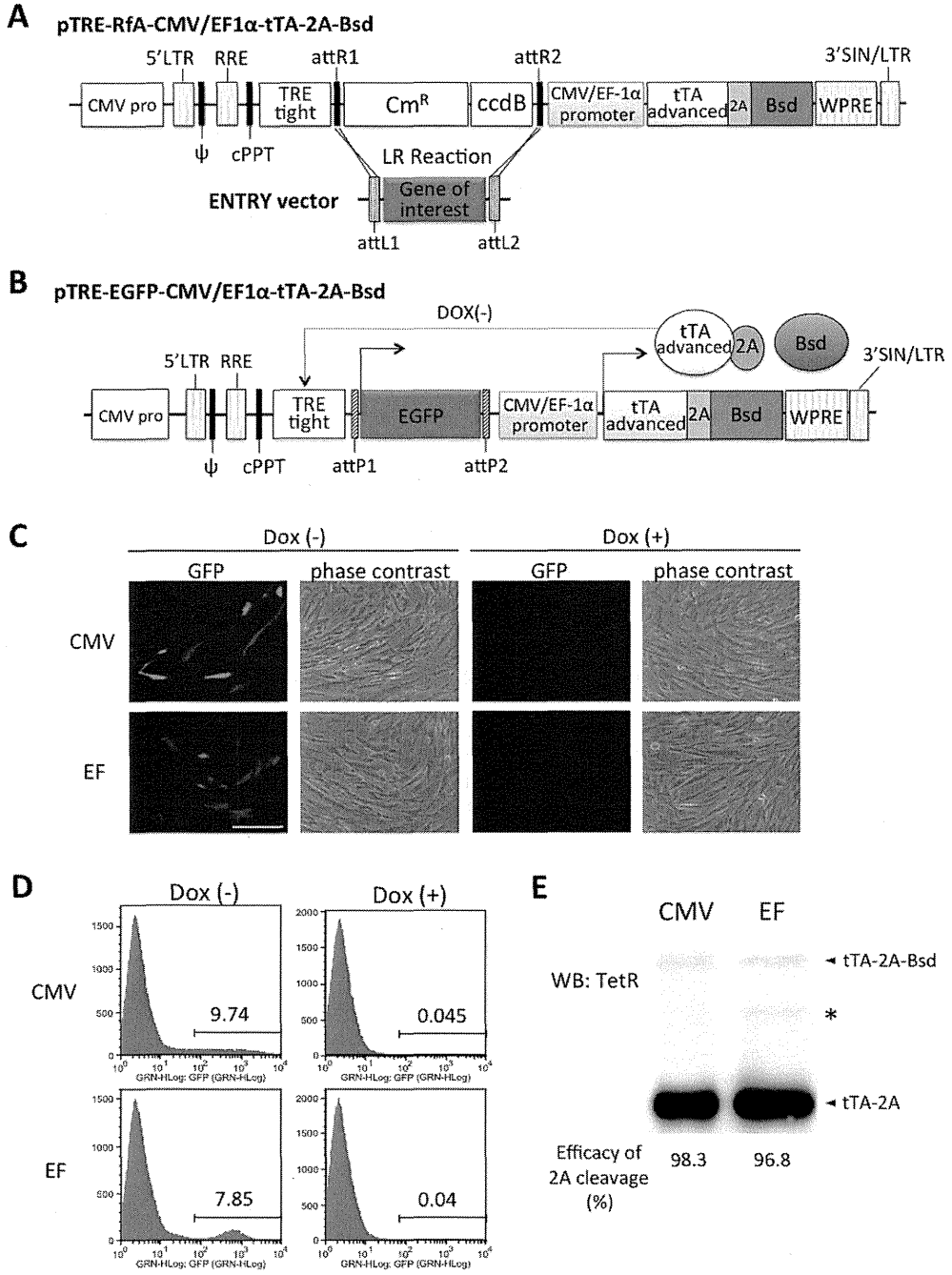

Figure 2. Schematic drawings of the single lentiviral vectors for tet-off system used in this work. (A) Gateway-compatible destination vectors containing *att*R recombination sites flanking a *ccd*B gene and a chloramphenicol-resistance gene, which allows an easy and rapid shuttling of gene of interest flanked by attL sites into the destination vectors using the Gateway LR recombination reaction. They also have an improved version of tetracycline-controlled transactivator (tTA) linked to the blasticidin resistant (Bsd) gene by the Thosea asigna virus 2A (2A) peptide sequence, whose expression is regulated by the CMV or EF-1α promoter. In the present study, we constructed an entry vector encoding EGFP flanked by attL, resulting in a destination clone, pTRE-EGFP-CMV-tTA-2A-Bsd or pTRE-EGFP-EF-tTA-2A-Bsd (B). In the absence of doxycycline (Dox), tTA-2A binds to the TRE-Tight promoter and activates EGFP transcription. For more details, see the Results section. CMV pro, CMV promoter; LTR, long terminal repeats; ψ, packaging signal; RRE, rev response elements; cPPT, central polypurine tract; TRE, tet-responsive element; Cm^R, chloramphenicol resistance; tTA, tetracycline-controlled transactivator; Bsd, blasticidin resistance; WPRE, woodchuck hepatitis virus posttranscriptional control element; SIN, self-inactivating. (C) (D) hADMPCs were transduced with pTRE-EGFP-CMV-tTA-2A-Bsd or pTRE-EGFP-EF-tTA-2A-Bsd at m.o.i. of 250. Four days after transduction, the cells were divided into 2 populations; with 1 μg/mL of Dox (Dox (+)) and without Dox (Dox (-)). (C) Fluorescent and phase contrast images. Scale bar, 200 μm. (D) Log fluorescence histograms of EGFP by flow cytometry analysis. (E) The whole cell lysates from hADMPCs transduced with pTRE-EGFP-CMV-tTA-2A-Bsd or pTRE-EGFP-EF-tTA-2A-Bsd were subjected to western blotting to monitor the cleavage efficiency of tTA-2A-Bsd proteins. A primary antibody against TetR was used to detect either tTA-2A-Bsd (non-cleaved form) or tTA-2A (cleaved form). Asterisk indicates a nonspecific band.

doi:10.1371/journal.pone.0066274.g002

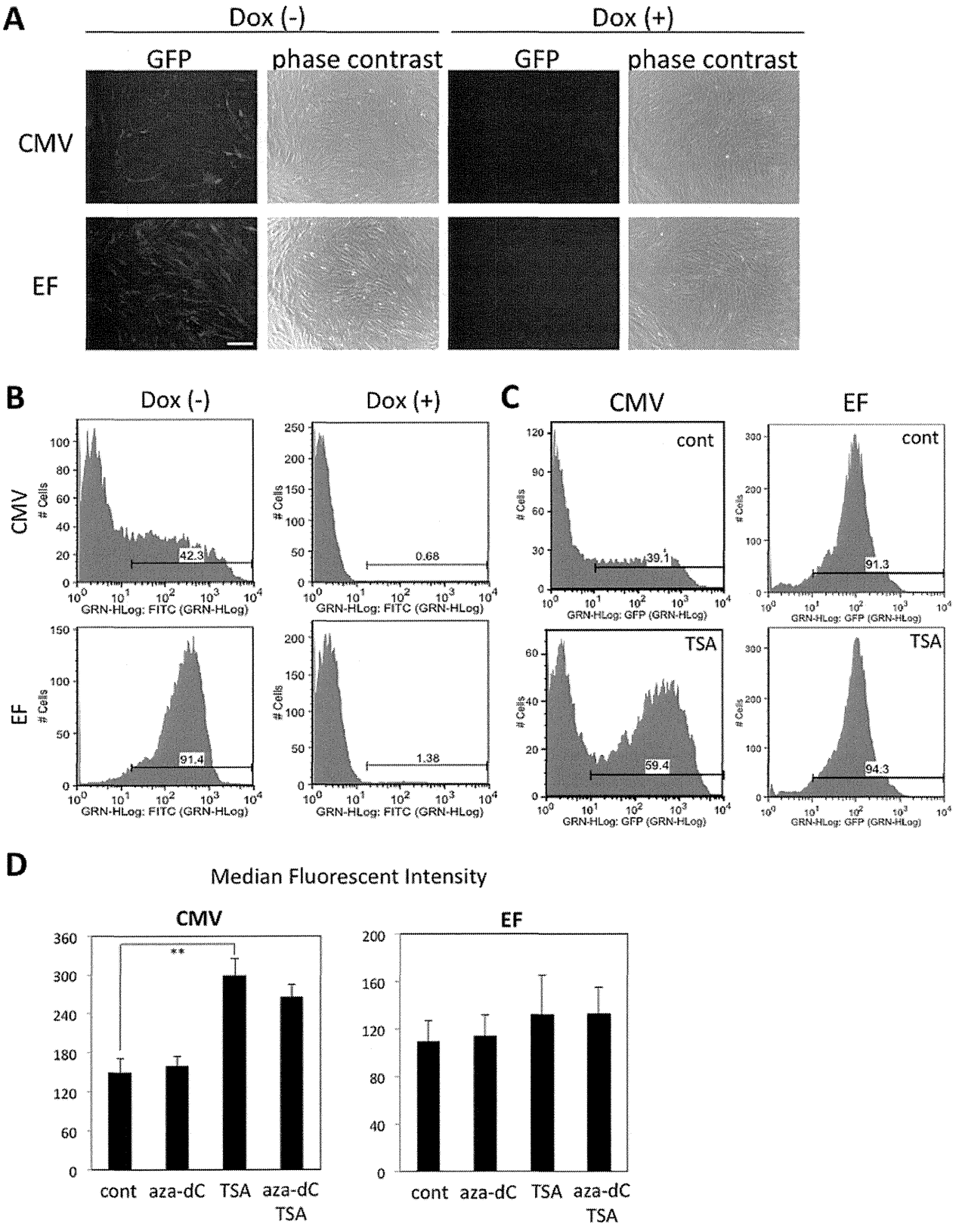

Figure 3. Blasticidin selection of hADMPCs transduced with single tet-off lentiviral vector platform. hADMPCs were transduced with pTRE-EGFP-CMV-tTA-2A-Bsd (CMV) or pTRE-EGFP-EF-tTA-2A-Bsd (EF) at m.o.i. of 250. The cells were treated with 4 μg/mL blasticidin and 1 μg/mL Dox for 2 weeks. Then, the cells were cultured in the absence (Dox (-)) or presence (Dox (+)) of 1 μg/mL Dox for 4 days, and analyzed under a microscope (A) and flow cytometer (B). The cells were treated with 100 nM TSA (TSA), 5 μM 5-aza-dC (aza-dC), or both for 48 h before analyzed by flow